

A new approach to possible substrate binding mechanisms for nitrile hydratase

A. Özlem Taştan Bishop^{a,b,*}, Trevor Sewell^c

^a Department of Biotechnology, University of the Western Cape, Bellville 7535, South Africa

^b Department of Biochemistry, University of Pretoria, Pretoria 0002, South Africa

^c Electron Microscopy Unit, University of Cape Town, Rondebosch 7701, South Africa

Received 29 January 2006

Available online 6 March 2006

Abstract

We combined normal mode analysis (NMA) with cavity calculations as a method to get more insight into static crystal structures. We used nitrile hydratase (NHase) as a case study, and the crystal structure of a complex of *Pseudonocardia thermophila* NHase (1UGP) with *n*-butyric acid was chosen as a reference structure. The reference structure was compared with the other available NHase crystal structures. Cavity calculations of the static structures showed the entrances to the active site and also a possible function of the N-terminal in the substrate selection of the Co-type NHase. When NMA was combined with cavity calculations, a closing–opening passage was observed. Analysis of low frequency modes combined with cavity calculations led us to propose “breathing” and “flip-flop” mechanisms which might be a key part of the substrate binding mechanism.

© 2006 Elsevier Inc. All rights reserved.

Keywords: NHase; Substrate binding mechanism; Breathing; Flip-flop; Normal mode; Cavity

With the advances in X-ray crystallography, many protein structures have been determined in detail. However, these static crystal structures need to be combined with other methods, such as biochemical data, in order to explain the functions of dynamic proteins. Additionally, various computational programs give rich insights into structural functional relationships. Normal mode analysis (NMA) is an important tool for understanding the flexibility of a protein. Another tool is the characterization of pockets and cavities in proteins, in order to determine potential sites for the binding of ligands, other proteins, and drugs. The complex shape of a protein provides a perfect environment for the binding of biologically functional ligands, normally around the active site, leading to catalysis. What if we combine normal mode analysis with cavity calculations? Does this lead us to a position where we can suggest how the substrate moves on the protein of interest?

As a case study, one of the available nitrile hydratase (NHase) structures is chosen. NHases catalyze the conversion of nitriles into their corresponding amides. These enzymes have been the subject of interest for both academia and industry for over two decades, mostly due to their biocatalytic activity (e.g., acrylamide and nicotinamide production) [1]. Also, their importance extends into usage for environmental remediation by being effective in removal of nitriles from waste streams [2].

NHase comprises two subunits, α and β , which are not related in the amino acid sequence, each with a molecular mass of around 23 kDa [3]. It is a soluble metalloenzyme that contains iron (Fe) or cobalt (Co) in its catalytic center. Thus, NHase is divided into two subgroups based on the co-factor requirement. The Fe-type NHase contains a single non-heme Fe^{III} per $\alpha\beta$ -dimer, while the Co-type NHase contains a single non-corrin Co^{III} per $\alpha\beta$ -dimer.

Many studies of the enzyme have been carried out since the first discovery of a NHase from an *Arthrobacter* bacterium by Asano et al. [4]. However, we are still far from understanding the molecular basis for NHase specificity

* Corresponding author.

E-mail address: ozlem@tuks.co.za (A.Ö. Taştan Bishop).

and activity. Up to date, there are four main papers describing the crystal structures of Fe-type [5,6] and Co-type NHases [7,8]. Recently, Miyanaga et al. [9] reported a combination of biochemical and structural results. Desai et al. [10] investigated substrate selectivity and reported the entrance numbers in Co- and Fe-type NHases (although their locations are not described). While the active site structure of NHase has been defined, a number of unanswered questions have yet to be addressed to understand this enzyme better, so as to be able to use it in industrial applications. Substrate specificity is an important issue. Different NHases are specific for different nitrile substrates. To understand how the protein selects the substrate and where the substrate binds may lead to a genetically engineered NHase producing organism which is non-specific to the nitrile substrate. This would make life very easy for industrial applications.

Generally, it might be useful to compare cavity volume with substrate volume, to get an idea if the substrate fits into the cavity. Also, measuring the size of the cavity mouth in the static crystal structure might provide some information on substrate accessibility. However, there is no doubt that the protein itself and the mouth opening are flexible, and static measurements help only to some extent. Here, in order to get more insight, we combine NMA with cavity calculations to take us one step closer towards determining possible NHase substrate binding mechanisms.

Materials and methods

Comparison of the structures. The coordinates of NHases from *Pseudonocardia thermophila* (1IRE and 1UGP), *Rhodococcus* sp. N-771 (2AHJ), and *Bacillus smithii* (1V29) were downloaded from the Protein Data Bank. The Align program was used to align available NHase PDB files into the coordinate system of the *P. thermophila* [11]. After superpositioning of PDBs by alignment, a detailed comparison was done with the program PyMOL [12].

Normal mode analysis and cavity calculations. NMA of NHase was performed using eINémo, a web interface to the Elastic Network Model [13]. The web server can be freely accessed at <http://igs-server.cnrs-mrs.fr/elnetmo/index.html>. One major application of NMA is the identification of potential conformational changes. eINémo assumes that the atoms in a molecule behave as simple harmonic oscillators. Thus, all of the possible motions of the molecule can be described by combinations of these oscillations. Directions of the oscillations are the normal modes which describe a harmonic oscillation of the structure about a local energy minimum.

Pocket and cavity volumes were computed by CASTp [14]. For all our calculations, a probe radius of 1.4 Å (the server default radius) was used. CASTp defines the pockets as empty concavities on a protein surface into which solvent can gain access. These concavities have mouth openings connecting their interior with the outside bulk solution. A cavity, on the other hand, is an interior empty space that is not accessible to the solvent probe. It has no mouth openings to the outside bulk solution. However, this distinction between cavity and pocket is not used uniformly in the literature, and for simplicity we will use the word “cavity” for both terms.

The CASTp results were compared with two other programs, namely, VOIDOO [15] and Q-SiteFinder [16]. Each of these cavity detection programs measures different kinds of cavity volumes so the volume results are not directly comparable. Instead, the rough locations of the volumes were compared. CASTp uses an α -shape-based procedure to measure the cavity

enclosed by the molecular surface of atoms that surround the cavity. VOIDOO is a grid-based procedure that measures the cavity volume defined by the van der Waals surface of atoms lining the cavity. In these programs, geometric criteria are used to define the location and extent of the pocket. The probe radius was 1.2 Å for the VOIDOO calculations. We also wanted to use another approach to check the reliability of the results. For this purpose Q-SiteFinder was ideal, in which the pockets are defined only by energetic criteria. The program calculates the van der Waals interaction energies of a methyl probe ($-\text{CH}_3$) with the protein.

The web pages of the programs are: CASTp, <http://cast.engr.uic.edu/cgi-bin/cast1/index.pl>; VOIDOO, <http://x-ray.bmc.uu.se/usf/voidoo.html>; Q-SiteFinder, <http://www.bioinformatics.leeds.ac.uk/qsitefinder>.

Results and discussion

Cavity calculations for a static view of NHase

The *P. thermophila* NHase (1UGP) is chosen as the reference structure for this work since this enzyme is the only available crystal structure of a complex with an inhibitor (*n*-butyric acid) that is up to date. The PDB file without this inhibitor is 1IRE. It is proposed that NHase is in the heterotetramer form in vivo [17]. For this reason, as a starting point for the cavity calculations, the heterotetramer form of the enzyme is used.

The surface representation of the $(\alpha\beta)_2$ -heterotetramer of *P. thermophila* NHase yields a number of cavities. For cavity calculations, the program CASTp gave 123 cavities. The ones that are selected for the further analysis and their cartoon representations are shown in Fig. 1. The data concerning cavity volumes and mouth opening sizes are summarized in Table 1. Although the calculations were done for the heterotetramer, analysis was focused on the heterodimer since the results are symmetric. Cavities 1 (cavities 1a and 1b), 4, and 5 are near to, or surrounding, the active site center; although in the static view cavities 1a and 1b are joined and named cavity 1, in some later analysis they are separate. Cavity 2 (cavities 2a and 2b) is the equivalent of cavity 1 in the other heterodimer and was chosen so that cavities 1 and 2 can be compared in the NMA. Cavity 3 is the cavity between two heterodimers and was chosen because NMA shows that it may be an opening (discussed below).

Cavity 1 is lined by residues or partial residues Thr2, Arg7, Asp10, Ile13, Gln14, Gln89, Leu110, Cys-SO₂H111, Ser112, Cys-SOH113, Tyr114, Trp116, Leu121, Pro122, Asn124, Trp125, Lys127, Glu128, Pro129, Gln130, and Arg132 from α -subunit; β -subunit ones are Tyr5, Gly12, Leu13, Gly14, Pro15, Asn17, Pro19, Glu22, Arg26, Ala27, Trp29, Glu30, Phe34, Phe37, Leu48, Phe51, Arg52, Ile55, Glu56, Tyr63, Leu64, Glu65, Ser66, Pro67, Tyr68, Tyr69, His71, Trp72, and Arg157. The residues from the other heterodimer are Leu6 α , Asn59 β , Pro60 β , and Ala61 β . Cavity 3 is lined by β -subunits from each heterodimer. On both sides the residues are Asn2, Asp6, Gly8, Gly9, Thr10, Arg146, Thr149, Ser151, Arg160, Tyr161, Arg163, Gly164, Lys165, Glu202,

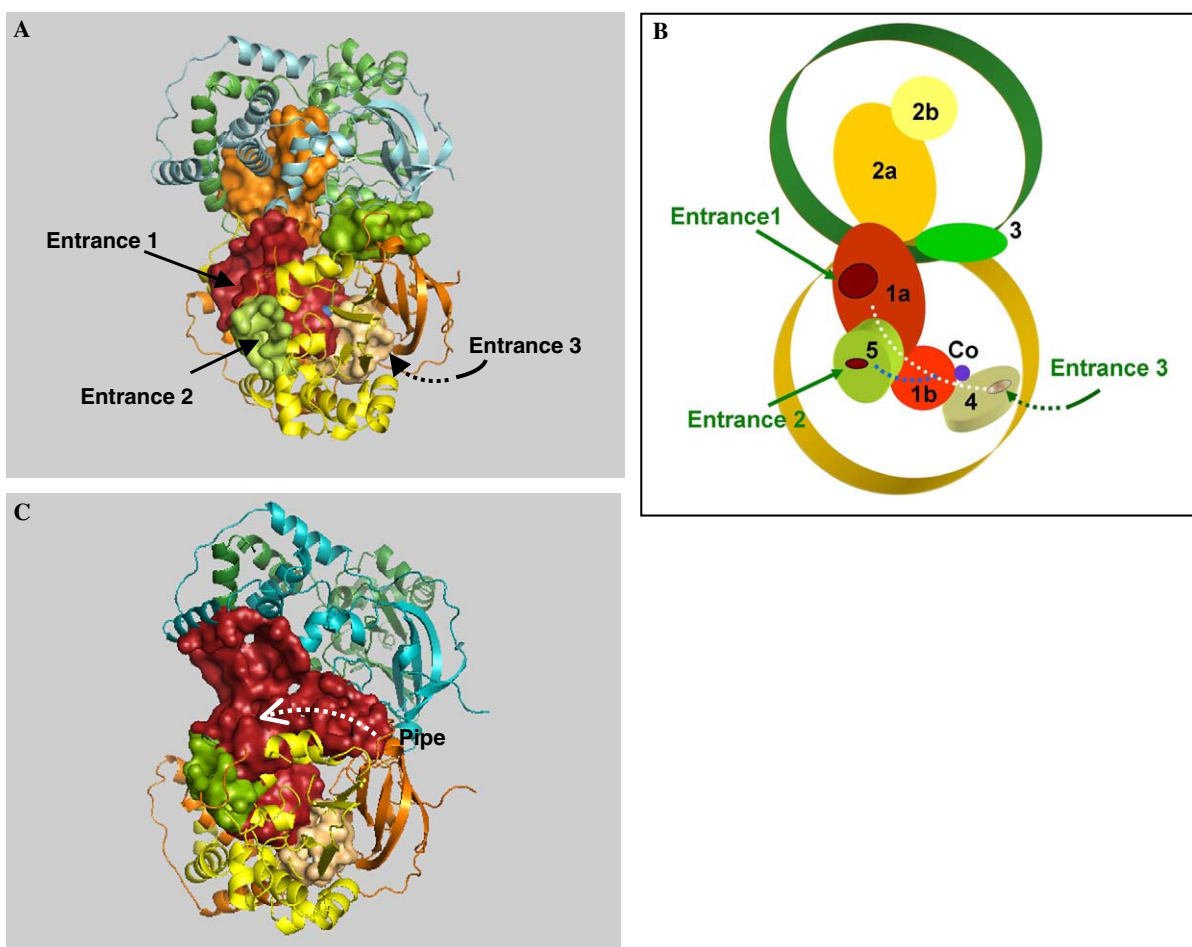


Fig. 1. (A) Cavities selected for the calculations. (B) Schematic representation of the cavities, numbered from 1 to 5. Some of the normal modes split the cavity which contains the entrance 1 into two, thus it is numbered as 1a and 1b. Three entrances to the channel are shown by arrows. The blue sphere is the Co atom. (C) Cavities for 1V29; the white arrow shows the location of the pipe. (For interpretation of the references to color in this figure legend, the reader is referred to the web version of this paper.)

Table 1
Volumes and mouth sizes of specified cavities in the static case, as well as for the end states of two normal modes, for the reference structure

		Static	Mode 1a	Mode 1b	Mode 2a	Mode 2b
Cavity 1 (a+b)	Volume	1584.68	1513.24	1668.03		2652.38
Entrance 1	Mouth	88.51	88.62	90.66		192.71
Cavity 1a	Volume				1090.01	
Entrance 1	Mouth				90.09	
Cavity 1b	Volume				528.85	
	Mouth				0	
Cavity 2	Volume	1584.76	1513.17	1667.96	2652.02	1089.97
	Mouth	88.22	89.32	93.18	172.14	91.32
Cavity 3	Volume	937.93	977.59	1196.89	944.41	944.36
	Mouth	54.01	55.42	66.17	52.48	51.54
Cavity 4	Volume	491.76	497.26	498.78	492.35	492.36
Entrance 3	Mouth	26.92	30.21	26.49	30.41	27.65
Cavity 5	Volume	471.33	467.21	482.13	477.07	477.04
Entrance 2	Mouth	55.94	53.54	56.22	56.77	56.75

CASTp computes parameters for both solvent accessible surface and molecular surface (MS), and the Table gives only the MS parameters.

Leu203, and Trp204. Cavity 4 is lined by Leu88, Gln89, Glu91, Asp92, Cys-SOH113, Ser163, Ser164, and Glu165 of α -subunit residues; Phe37, Phe41, Leu48, Asp49, Arg52, Leu127, Pro128, Ala129, Arg131, His155, Arg157, Tyr176, Ile177, Pro179, Leu193, and Trp219 of β -subunit. Cavity 5 has Tyr46, Val50, Gly51, Pro52, Leu119, Gly120, Leu121, Pro122, Pro123, Asn124, Trp125, Lys127, Arg192, and Glu193 from α -subunit and Arg18, Pro19, Ala20, Asp21, Glu22, Pro23, Val24, Arg26, Glu30, Tyr68, and Tyr69 from β -subunit.

CASTp calculations showed that the channel to the active site has three entrances (Figs. 1 and 2), which we name entrance-1 (which leads into cavity 1), entrance-2 (into cavity 5), and entrance-3 (into cavity 4). It is possible to observe the substrate *n*-butyric acid through entrance-2 and entrance-3 (Fig. 2).

The cavity calculations were repeated using the programs VOIDOO and Q-SiteFinder. In all cases, cavities 1, 2, and 3 were found to be the largest cavities with locations approximately as found by CASTp. However, the programs did not all agree concerning the smaller cavities. A comparative study of CAST and VOIDOO was reported earlier, and it was shown that VOIDOO had difficulty detecting small cavities located close to the surface [18]. Q-SiteFinder showed that the smaller cavities were not distributed evenly between two heterodimers of the heterotetramer, and thus these results cannot be considered significant.

Comparison of the static views of NHases

An interesting observation comes from a comparison of the heterotetramer form of the reference structure with

other structures. In structure *B. smithii* (1V29), although the first 14 residues are missing, the N-terminal of the α -subunit of each heterodimer still extends into a position where the entrance-1 of the other heterodimer is located and almost blocks the entrance-1 (Fig. 3B). On the other hand, in the reference structure, the N-terminal of the α -subunit, for which we have complete information about the location of all N-terminal residues, does not extend to the other heterodimer; thus, it does not block the entrance-1 to the cavity (Fig. 3A). In the heterodimer forms of both reference case and *B. smithii* (1V29), some active site residues (Cys-SO₂H111 α and Ser112 β) can be seen through entrance-1. This is true for the heterotetramer form of the reference structure but not for *B. smithii* (1V29), since entrance-1 is almost blocked by the dimerization. This extended N-terminal leads to different CASTp results for *B. smithii* (1V29) than for the reference structure. It gives one volume that includes cavity 1 and cavity 3, that is two cavities joined by a pipe (Fig. 1C).

This major structural difference between two Co-type NHases from two different organisms might play an important role in ligand selection criteria. The NHase from *B. smithii* prefers aliphatic nitriles as substrate rather than aromatic ones, contrary to *P. thermophila* [8,19]. Additionally, Miyanaga et al. could soak *n*-butyric acid into the reference crystal perhaps due to the short N-terminal arm leaving the entrance-1 wide open; it is interesting here that successful soaking has not been reported for the other crystal structure, possibly because entrance-1 is almost blocked.

When the comparison is extended to the Fe-type NHase from *Rhodococcus* sp. N-771 (2AHJ), very similar features

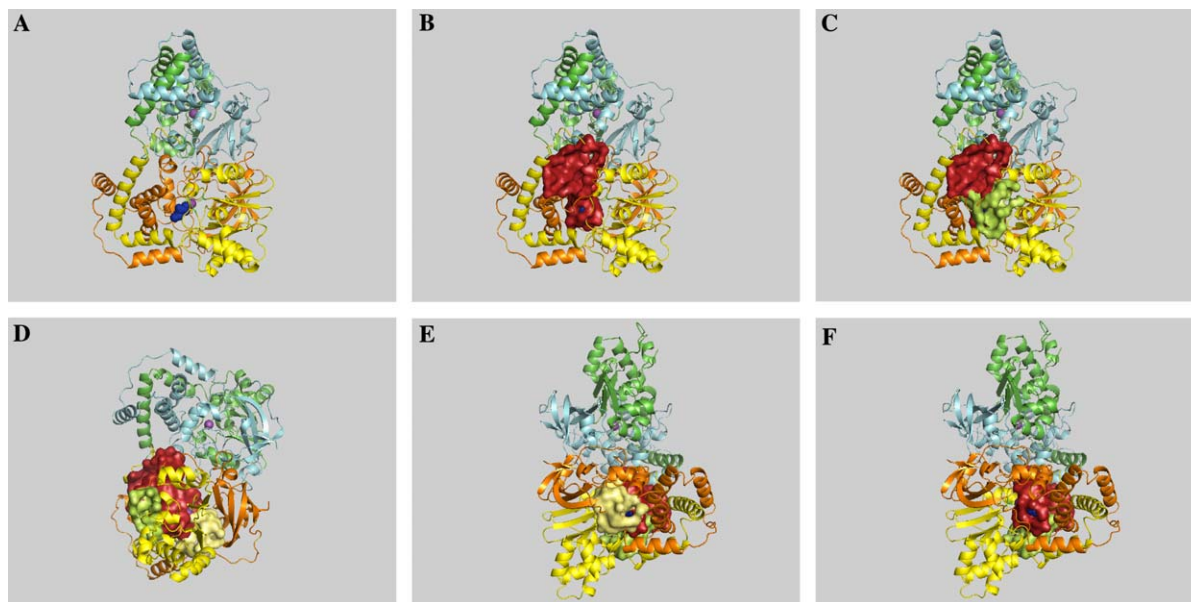


Fig. 2. (A) Cartoon representation of UGP with *n*-butyric acid (blue spheres) and Co atom (violet sphere) located in one of the heterodimers. (B) Cavity 1 and the passage between cavity 1 and cavity 5; *n*-butyric acid can be observed. (C) Cavity 5 where *n*-butyric acid can be still observed. (D) Location of cavity 5 and the cobalt atom between cavity 1 and cavity 4. (E) Entrance 3 through cavity 4 and *n*-butyric acid. (F) Passage between cavity 1 and cavity 4. (For interpretation of the references to color in this figure legend, the reader is referred to the web version of this paper.)

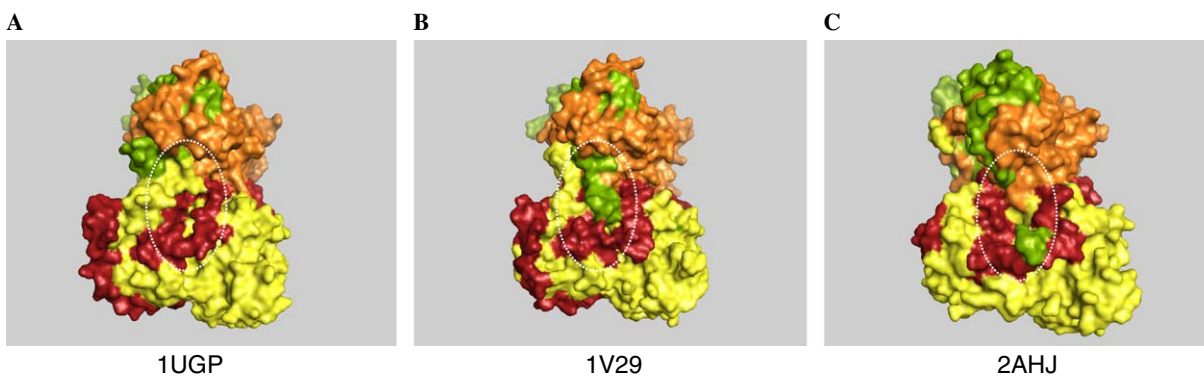


Fig. 3. Comparison of the location of the N-terminal, shown in green, of the α -subunit in three different available crystal structures. The white elliptical mark shows how it extends, in two cases, to the other heterodimer. (For interpretation of the references to color in this figure legend, the reader is referred to the web version of this paper.)

to *B. smithii* (1V29) were observed even though information about the missing residues (6–12) prevent a complete view (Fig. 3C). However, an interesting point is that in the region where the N-terminal extends there is no entrance to a channel. The channel has only one entrance, equivalent to entrance-3 in the reference structure.

Normal mode analysis

The heterodimer and heterotetramer forms of the reference structure were deposited into the EInémo web page for the NMA calculations. The program computes the 100 lowest frequency modes. The results of the heterotetramer were more informative, and the first five modes were considered. Generally all five modes showed that NHase has a very rigid body, and no major opening was observed. The end states of these modes were saved as new PDB files, and cavity calculations were performed.

Interestingly, in most of the modes there is a passage between cavity 1 and cavity 5 that is open in one end state and closed in the other end state (Fig. 4, Table 2). The open form of the passage in the first mode was analyzed. The residues, or partial residues, located at the mouth of this passage are Leu121 α , Pro122 α , Lys127 α , Tyr68 β , and Tyr69 β . Also, the residue Trp72 β is located very near to the passage mouth and is conserved in all Co-type NHases. The amino acid corresponding to this residue in Fe-type NHases is Tyr76 β , and it is thought that it might be important for substrate binding [7].

The importance of Tyr68 β was mentioned by Miyanaga et al. [9]. They demonstrated that the mutant shows a significant decrease in activity compared to the wild type enzyme, although the crystal structure of the mutant is almost identical to that of the wild type except at the mutation site. Additionally, they reported that the K_i value for *n*-butyric acid is approximately 10 times higher than that of the wild type enzyme. They propose that this residue stabilizes the imidate intermediate and the claw setting of the active site [9]. The NMA results described above show that it may be that Tyr68 β has an important function in the opening and closing movement of the passage, thus

controlling substrate selectivity through the passage between channel 1 and 5, and entrance-2.

In order to compare the reference structure with *B. smithii* (1V29) and *Rhodococcus* sp. N-771 (2AHJ), normal modes of these two structures were also obtained. A difference in the region of cavity 3 was observed, wherein the static case the structures are almost identical. In the reference case and 2AHJ, that area is quite rigid in all the modes analyzed; but in the case 1V29, there is some flexibility and an entrance into cavity 3 opens. As we discussed in the previous section, there is a pipe connecting cavity 3 with cavity 1 and leading to the active center.

Possible substrate binding mechanisms

Analysis of each normal mode, and cavity calculations for the end states of these modes, gave a number of insights. We proceeded by investigating the two lowest frequency modes and looking at how cavities in the end states differ from the cavities in the static case. The data for this discussion presented in Table 1.

Cavity 1 in mode 2 has the largest change in volume and mouth size, the mouth being entrance 1. At the minimum the cavity pinches into two parts, cavities 1a and 1b. In this mode when cavity 1 is a minimum, cavity 2 is a maximum and vice versa. The other cavities do not change significantly in this mode. Thus, mode 2 can be described as a flip-flop mechanism involving cavities 1 and 2.

In mode 1, there are changes of the order of up to 10% in the volume or entrance size for cavity 1 and entrance 1, cavity 4 and entrance 3, and cavity 5 and entrance 2. All these changes happen in phase, so this mode of vibration can be described as a breathing mechanism.

Although we distinguish between breathing and flip-flop mechanisms, from the point of view of the possible motion of the substrate they are equivalent, because they both involve opening and closing of entrances and channels, as well as volume changes of the cavities.

An alternative mechanism for *B. smithii* (1V29) may be that an entrance opens into cavity 3, which is connected to cavity 1 by a pipe, as discussed in Normal mode analysis.

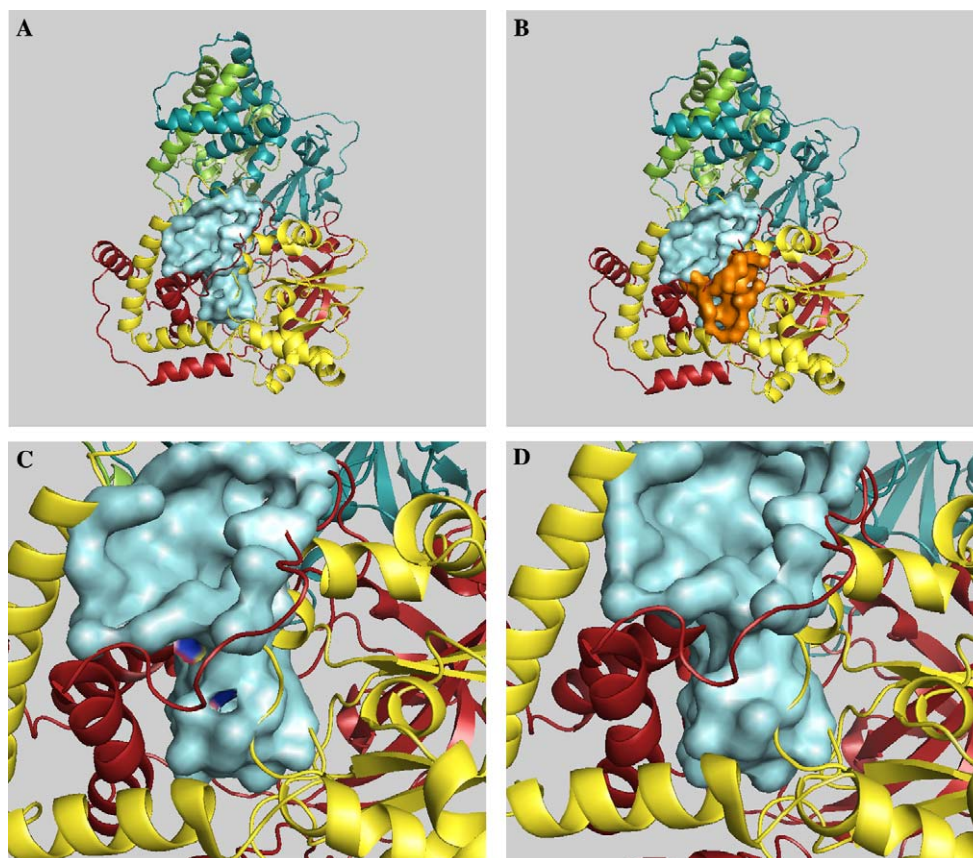


Fig. 4. (A) Cavity 1 in open state. (B) Passage between cavity 1 and cavity 5 can be clearly seen. (C) Closer view of the open form of the passage. The blue color in the passage indicates the location of the residue Y68 β and the pink color the residue Tyr72 β . (D) Closed form of the passage. (For interpretation of the references to color in this figure legend, the reader is referred to the web version of this paper.)

Table 2
Status of the passage between cavities 1 and 5 in the end states of different normal modes

Normal modes	Passage between cavity 1 and cavity 5
Mode 1a	Open
Mode 1b	Closed
Mode 2a	Open
Mode 2b	Slightly open
Mode 3a	Open
Mode 3b	Closed
Mode 4a	Closed
Mode 4b	Slightly open
Mode 5a	Closed
Mode 5b	Closed

Conclusion

Static crystal structure is not enough to explain dynamic protein function. In this paper, we propose to combine two different approaches which study protein function from different aspects, namely normal mode analysis and cavity calculations. Application of this combined approach to the available crystal structures of the NHases from differ-

ent organisms led to a comparison of the differences and to a number of conclusions.

Analysis of the static view of the reference structure, and the other available structures, showed various cavities which lead to the active site and the entrances to these cavities. Co-type NHases have three entrances to the active site channel while Fe-type NHase has only one. Interestingly, the N-terminal of the α -subunit in *B. smithii* (1V29) structure almost blocks one of the entrances. Extension of the N-terminal might be relevant to substrate specificity; if this idea were correct, then it would follow that soaking the substrate into 1V29 crystals would not be successful. Also, this extension of the N-terminal causes different results in cavity calculations. Two separate cavities in the reference structure are combined in the 1V29 structure into a form like a pipe, which shows flexibility in NMA. This leads to a possible substrate binding mechanism for 1V29 resulting from the opening and closing of an entrance into cavity 3; this distinct opening was not observed in any of the other cases. For the reference structure, the possible substrate binding mechanisms are breathing and flip-flop, involving the opening and closing of the cavities and mouths. Also, a passage between cavity 1 and cavity 5 was observed. This passage opens in one end state and closes in the other end state of most of the normal modes. The residue Try68

located in this passage might be important for substrate selection.

Generally, we believe that this combined approach can be applicable to any crystal structure and result in more information about functional aspects.

Acknowledgments

AÖTB was supported, at different times, by National Research Foundation, South Africa, and by the Claude Leon Foundation. The idea for this paper arose during other work done in collaboration with Prof. D. Cowan and Dr. M. Sayed. We thank Prof. N.T. Bishop for editing; Dr. B. Weber for discussion; J. Watermeyer for assistance with certain programs and references; Dr. J. Dundas for assistance with CASTp; Dr. G. Kleywegt for assistance with VOIDOO; and Dr. A. Laurie for assistance with Q-SiteFinder.

References

- [1] H. Yamada, M. Kobayashi, Nitrile hydratase and its application to industrial production of acrylamide, *Biosci. Biotechnol. Biochem.* 10 (1996) 1391–1400.
- [2] J.M. Wyatt, C.J. Knowles, Microbial degradation of acrylonitrile waste effluents: the degradation of effluents and condensates from the manufacture of acrylonitrile, *Int. Biodeter. Biodegrad.* 35 (1995) 227–248.
- [3] M. Kobayashi, T. Nagasawa, H. Yamada, Enzymatic synthesis of acrylamide: a successful story not over yet, *Trends Biotechnol.* 10 (1992) 402–408.
- [4] Y. Asano, K. Fujishiro, Y. Tani, H. Yamada, Aliphatic nitrile hydratase from *Arthrobacter* sp. J-1. Purification and characterization, *Agric. Biol. Chem.* 46 (1982) 1165–1174.
- [5] W. Huang, J. Jia, J. Cummings, M. Nelson, G. Schneider, Y. Lindqvist, Crystal structure of nitrile hydratase reveals a novel iron centre in a novel fold, *Structure* 5 (1997) 691–699.
- [6] S. Nagashima, M. Nakasako, N. Dohmae, M. Tsujimura, K. Takio, M. Odaka, M. Yohda, N. Kamiya, I. Endo, Novel non-heme iron center of nitrile hydratase with a claw setting of oxygen atoms, *Nat. Struct. Biol.* 5 (1998) 347–351.
- [7] A. Miyanaga, S. Fushinobu, K. Ito, T. Wakagi, Crystal structure of cobalt-containing nitrile hydratase, *Biochem. Biophys. Res. Commun.* 288 (2001) 1169–1174.
- [8] S. Hourai, M. Miki, Y. Takashima, S. Mitsuda, K. Yanagi, Crystal structure of nitrile hydratase from a thermophilic *Bacillus smithii*, *Biochem. Biophys. Res. Commun.* 312 (2003) 340–345.
- [9] A. Miyanaga, S. Fushinobu, K. Ito, H. Shoun, T. Wakagi, Mutational and structural analysis of cobalt-containing nitrile hydratase on substrate and metal binding, *Eur. J. Biochem.* 271 (2004) 429–438.
- [10] V.L. Desai, M. Zimmer, Substrate selectivity and conformational space available to bromoxynil and acrylonitrile in iron hydratase, *Dalton Trans.* 8 (2004) 72–877.
- [11] G.E. Cohen, ALIGN: a program to superimpose protein coordinates, accounting for insertions and deletions, *J. Appl. Cryst.* 30 (1997) 1160–1161.
- [12] W.L. DeLano, The PyMOL Molecular Graphics System on World Wide Web, <<http://www.pymol.org/>> (2002).
- [13] K. Suhre, Y. Sanejouand, ElNemo: a normal mode web server for protein movement analysis and the generation of templates for molecular replacement, *Nucleic Acids Res.* 32 (2004) W610–W614.
- [14] J. Liang, H. Edelsbrunner, C. Woodward, Anatomy of protein pockets and cavities: measurement of binding site geometry and implications for ligand design, *Protein Sci.* 7 (1998) 1884–1897.
- [15] G.J. Kleywegt, T.A. Jones, Detection, delineation, measurement and display of activities in macromolecular structures, *Acta Crystallogr. D* 50 (1994) 178–185.
- [16] A.T.R. Laurie, R.M. Jackson, Q-SiteFinder: an energy-based method for the prediction of protein-ligand binding sites, *Bioinformatics* 21 (2005) 1908–1916.
- [17] M. Nakasako, M. Odaka, M. Yohda, N. Dohmae, K. Takio, N. Kamiya, I. Endo, Tertiary and quaternary structures of photoreactive Fe-type nitrile hydratase from *Rhodococcus* sp. N-771: roles of hydration water molecules in stabilizing the structures and the structural origin of the substrate specificity of the enzyme, *Biochemistry* 38 (1999) 9887–9898.
- [18] S. Chakravarty, A. Bhinge, R. Varadarajan, A procedure for detection and quantitation of cavity volumes in proteins, *J. Biol. Chem.* 277 (2002) 31345–31353.
- [19] Y. Takashima, Y. Yamaga, S. Mitsuda, Nitrile hydratase from a thermophilic *Bacillus smithii*, *J. Ind. Microbiol. Biotechnol.* 20 (1998) 220–226.